Polymer 52 (2011) 3603–3610

Contents lists available at ScienceDirect

Polymer

journal homepage: www.elsevier.com/locate/polymer

Jet deposition in near-field electrospinning of patterned polycaprolactone and sugar-polycaprolactone core–shell fibres

Feng-Lei Zhou [a], Penny L. Hubbard [a], Stephen J. Eichhorn [b,*], Geoffrey J.M. Parker [a,**]

[a] Imaging Sciences, Biomedical Imaging Institute, Manchester Academic Health Sciences Centre, The University of Manchester, Manchester M13 9PT, UK
[b] School of Materials and the Northwest Composites Centre, Sackville Street, The University of Manchester, Manchester M13 9PL, UK

ARTICLE INFO

Article history:
Received 7 April 2011
Received in revised form
2 June 2011
Accepted 2 June 2011
Available online 13 June 2011

Keywords:
Jet deposition
Coaxial electrospinning
Polycaprolactone

ABSTRACT

In this work, the effects of process parameters on the deposition of single component and compound core–shell jets in near-field electrospinning are reported. It is shown that the working distance and fibre collector speed have a more significant influence on the deposition of a single jet than the flow rate. In the case of a compound jet, it is shown that jet deposition onto aluminium foil results in a linear fibre form, but on glass slides it appears as a random fibre network. The fabrication of aligned and patterned core–shell structured fibres is demonstrated by coaxial electrospinning of sugar and polycaprolactone (PCL) solutions. Aligned sugar-PCL core–shell fibres with diameters of ~1.2 μm are deposited on an *x*–*y* translation stage, 10 cm below the coaxial spinneret. Complex patterns of sugar-PCL core–shell fibres with average diameters ranging from 72 to 175 μm are fabricated by reducing the working distance to 2 cm.

1. Introduction

Electrospinning is a highly versatile technique to produce random or aligned micro or nanofibre assemblies from polymer solutions or melts [1,2]. The electrically charged fluid jet employed during electrospinning initially follows a straight path, and at a certain point breaks into a spiral trajectory (typically called the 'whipping instability'), while moving at a velocity of a few metres per second towards a grounded stationary collector, resulting in random nanofibre deposition [3–5]. Alignment of an electrospinning jet has been achieved by introducing an auxiliary electric field [6] or a magnetic field [7]. Rotating collectors have also been employed for this purpose [1]. More recently a fluid jet comprising only a straight segment has been reported in a process called near-field electrospinning [8,9]. This is achieved by setting the working distance between the spinneret and fibre collector to a position before the onset of the whipping instability. This technique allows the precise control of the deposition of the fluid jet onto a collector [10–12]. The application of an *x*–*y* translation stage has enabled the deposited fibres to find applications for chip connection [13] and energy harvesting [14]. However, there have been very few studies on the effect of process parameters involved in near-field electrospinning on jet deposition and fibre diameter, although the influences of collector speed and material type have been reported [12,15]. The effects of electrical, gravity and air drag forces have been theoretically simulated [16]. Moreover, no attempt has been made to investigate the precise deposition of a compound core–shell jet in near-field electrospinning, although the precise deposition of single component jet has been reported [10].

In recent years, the single needle spinneret system in a basic electrospinning setup has been modified to satisfy various practical requirements such as productivity enhancement [17] and the production of core–shell [18] or hollow fibres [19,20]. For core–shell and hollow fibres, a coaxial spinneret composed of an outer and inner needle is most commonly used; the process itself is known as coaxial electrospinning. With this kind of spinneret, coaxial electrospinning is able to fabricate, from various solution pairs, core–shell, hollow and functional fibres that may contain particles, and that may also have similar size ranges to non-coaxial electrospun fibres [21]. Fibres produced by coaxial electrospinning have found applications in drug delivery [22,23], as tissue engineering scaffolds [24], as templates and hosts for chemical reactions [25], and as a membrane separation in Li-air batteries [26]. The influence of

* Corresponding author. Tel.: +44 161 306 5982; fax: +44 161 306 3858.
** Corresponding author. Tel.: +44 161 275 5731; fax: +44 161 275 5145.
E-mail addresses: s.j.eichhorn@manchester.ac.uk (S.J. Eichhorn), geoff.parker@manchester.ac.uk (G.J.M. Parker).

0032-3861/$ – see front matter © 2011 Elsevier Ltd. All rights reserved.
doi:10.1016/j.polymer.2011.06.002

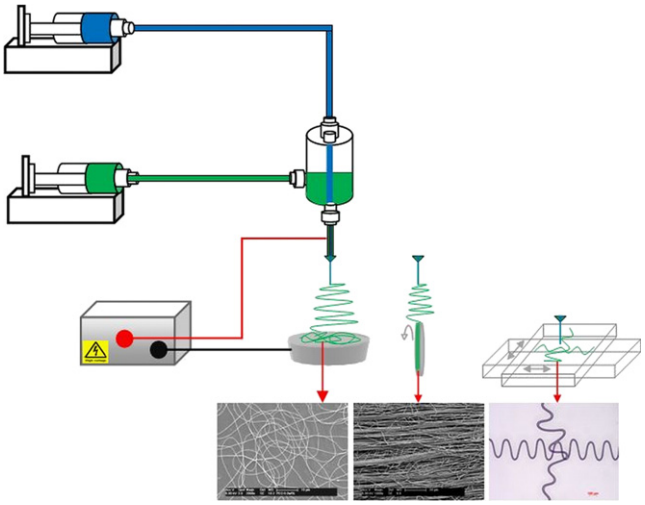

Fig. 1. Schematic of the coaxial electrospinning setup with stationary and mobile fibre collectors used to prepare core–shell microfibres. Core fluid shown in blue; shell fluid shown in green. Images show typical forms of fibres that can be achieved; random, aligned and patterned (left to right). (For interpretation of the references to colour in this figure legend, the reader is referred to the web version of this article.)

solvent type and the inner flow rate of the core materials has been reported [22,27–30]. There have been limited investigations of the production of core–shell fibre assemblies with well-defined alignment by coaxial electrospinning; to the authors' knowledge only two papers reporting alignment on parallel electrodes or rotating collectors have been published [31,32]. Aligned core–shell fibres are highly desirable for a number of applications including neural tissue engineering [33], controllable protein delivery systems [34] and as components in supercapacitors [35].

In this study, we report the controlled deposition of near-field electrospun polycaprolactone (PCL) single and sugar-PCL compound jets, motivated by our eventual aim to produce materials with microstructure similar to that seen in neuronal and muscle tissues. The effects of various near-field electrospinning parameters such as working distance, flow rate and x–y stage speed on the PCL single component jet deposition are reported and resultant fibre diameters are determined. The morphology of sugar-PCL compound jet deposited on glass slides and aluminium foil using the x–y stage are also reported. Finally, we produce patterned sugar-PCL core–shell fibres using an x–y translation stage in a near-field electrospinning configuration.

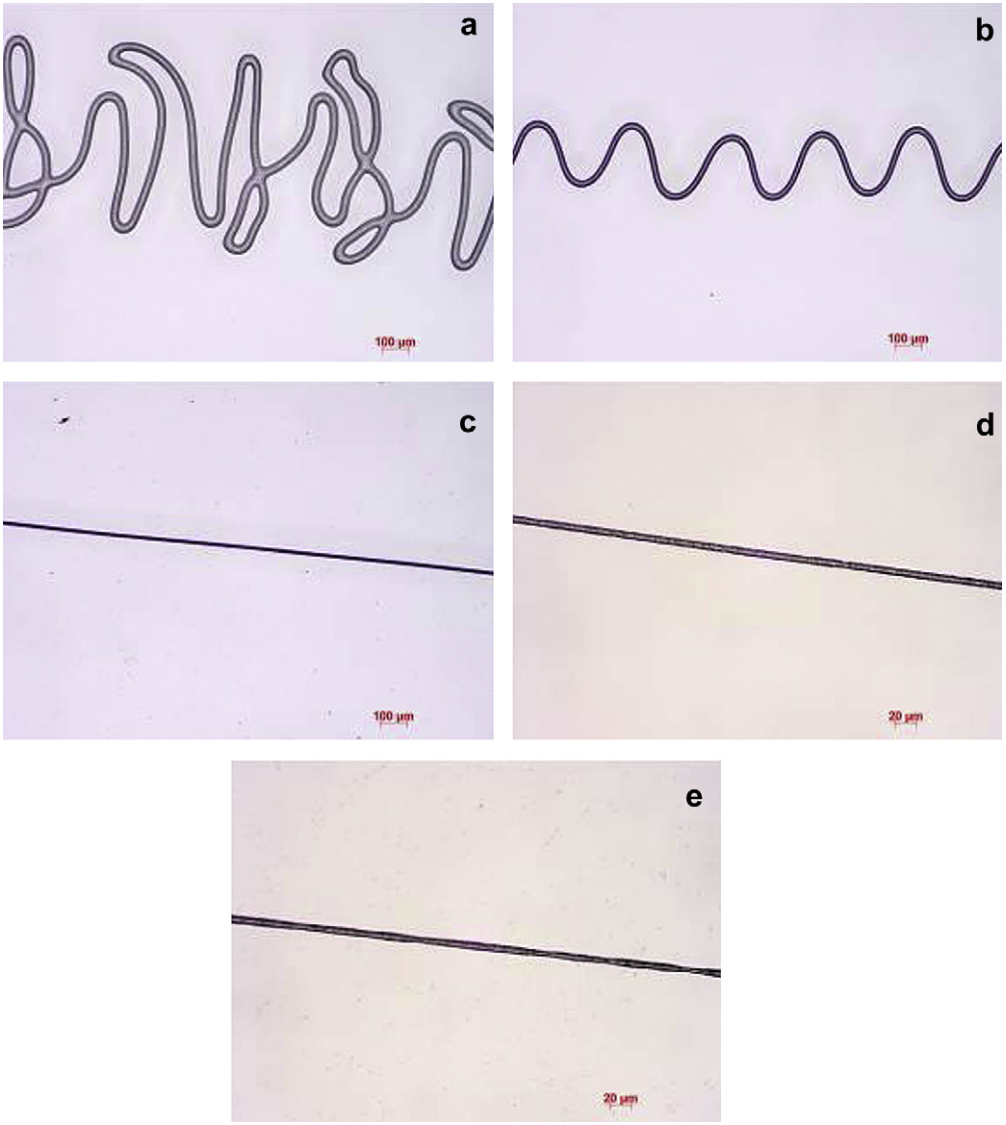

Fig. 2. Optical micrographs showing the effect of translation speeds (a) 20 mm s^{-1}, (b) 25 mm s^{-1}, (c) 30 mm s^{-1}, (d) 40 mm s^{-1} and (e) 45 mm s^{-1} on the form of the deposition of a jet of PCL. Experimental parameter settings: 2 kV applied voltage, 1 mm working distance, 0.06 ml h^{-1} flow rate. Scale bars in a-c and d–e: 100 and 20 μm, respectively.

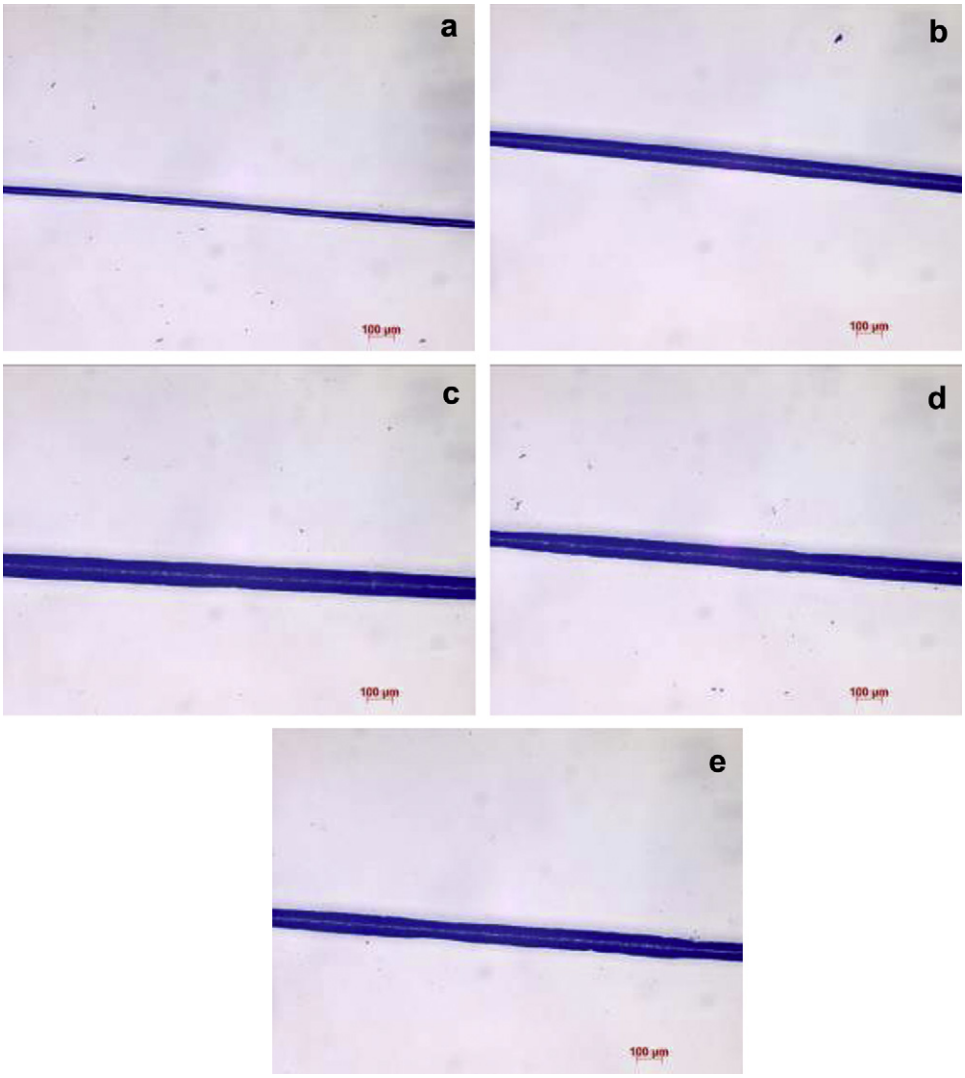

Fig. 3. Optical micrographs showing the effect of flow rates (a) 0.03 ml h^{-1}, (b) 0.06 ml h^{-1}, (c) 0.09 ml h^{-1}, (d) 0.15 ml h^{-1} and (e) 0.18 ml h^{-1} on single jet deposition. Experimental parameter settings: 4 kV applied voltage, 2 mm working distance, 30 mm s^{-1} translation speed. Scale bar: 100 μm. Note: the same electric field strength - 2 kV mm^{-1} was used in Figs. 2 and 3.

2. Experimental

2.1. Materials

Polycaprolactone (PCL, weight-average molecular weight M_W = 70,000–90,000 g mol^{-1}) was obtained from Sigma Aldrich (Dorset, UK) and used without further treatment or purification. Chloroform and N,N-dimethyl-formamide (DMF) solvents were also purchased from Sigma Aldrich (Dorset, UK). White table sugar, used for the sucrose solution, was purchased from a local supermarket. Deionised water was used to dissolve the sugar.

2.2. Coaxial electrospining setup

A schematic of the coaxial electrospining setup used for the production of core–shell fibres is shown in Fig. 1. The setup includes two syringe pumps (SP230IWZ, Multi-Syringe Pump, World Precision Instruments, UK and R-100E Single Syringe Infusion Pump, Sandown Scientific, UK) set to shell and core flow rates, and a high voltage power supply (PS/FC30R04.0–22, Glassman High Voltage, UK). An x–y translation stage was used for fibre collection. Two 10 ml syringes filled with the core fluid and shell fluid, respectively, were connected to a tubular stainless steel reservoir through PTFE tubes attached to luers (Cole–Parmer Instrument Co. Ltd., UK) that screwed into a steel reservoir. The reservoir had three luers, two of which were connected to two concentrically located stainless steel needles: a 22-gauge (OD 0.72 mm, ID 0.41 mm) inner needle and a 16-gauge (OD 1.65 mm, ID 1.19 mm) outer needle, respectively (ESSLAB, UK). The core and shell needles were locked into their respective luers, and then were threaded into the reservoir from the top and the bottom, which helped fix the needles in a concentric conformation. The third luer led into the reservoir from the side wall and provided an inlet for the shell fluid. The outer needle was connected to the positive electrode from the power supply, whereas the fibre collector, which was placed at a desired distance from the tip of the concentric needles, was connected to the negative electrode (ground). The inner needle was kept to an electrical potential that, depending on the conductivity of the outer fluid, was varied from that of the outer needle to that of the grounded plate. The coaxial electrospinning setup was placed in a fume cupboard.

10 wt% of PCL in chloroform/DMF (80/20, w/w) was used to investigate the PCL single jet deposition, where only the outer needle was used after removal of the inner needle. 50 wt% of sugar

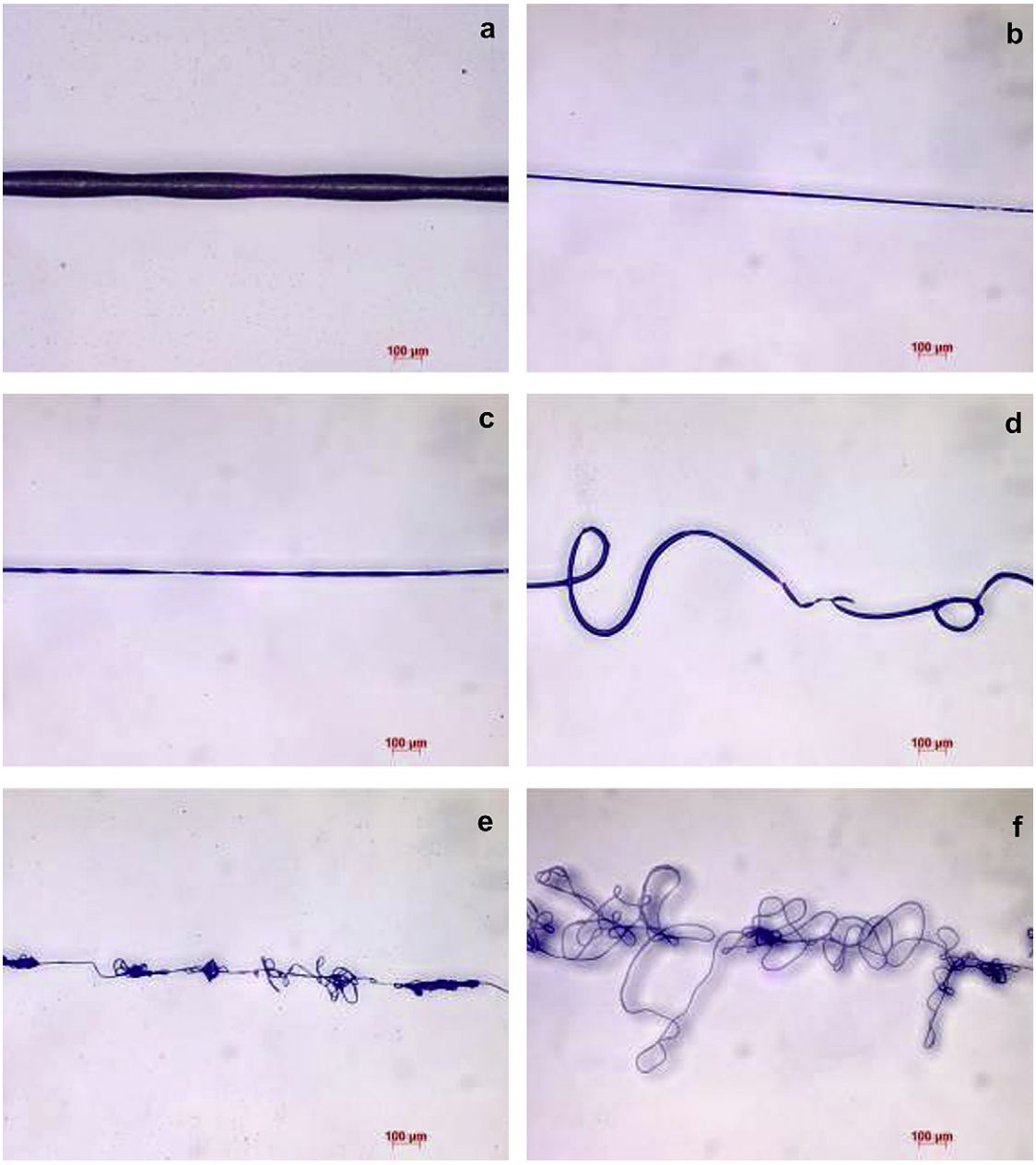

Fig. 4. Optical micrographs showing the effect of working distances (a) 1 mm, (b) 2 mm, (c) 3 mm, (d) 5 mm, (e) 7 mm and (f) 9 mm on the deposition of a single jet of PCL. Experimental parameter settings: 0.8 kV mm^{-1} electric field, 0.3 ml h^{-1} flow rate, 30 mm s^{-1} translation speed. Scale bar: 100 μm.

in deionised water and 10 wt% of PCL in chloroform/DMF (80/20, w/w) were used to produce the core and shell of sugar-PCL fibres, respectively.

2.3. Optical and electron microscopy imaging

The jet deposition and morphology of the fibres were studied using an Olympus BH2-UMA optical microscope and a JEOL 6300 scanning electron microscope (SEM) with an accelerating voltage of 5 kV. The surface morphology and cross-sections of as-spun core–shell sugar-PCL fibres were investigated using a Philips XL30 FEG SEM with an accelerating voltage of 5 kV. Image processing software ImageJ (NIH) was used to measure the fibre diameters from the SEM micrographs. For each sample, fibre diameters were measured at 90 different points within the SEM image field of view.

3. Results and discussion

3.1. Deposition of single PCL jet

3.1.1. Effect of translation speed

During the electrospinning process, a PCL jet was first deposited onto aluminium foil, and then a glass slide, along a pre-set trajectory using the x–y stage. The electrospinning jet remained steady and straight, even when the deposition crossed the boundary between the aluminium foil and the glass slide. Images of the jet deposition of PCL onto glass slides under various translation speeds are shown in Fig. 2. A single component PCL fibre was deposited in an undulating form when the translation speed was below 30 mm s^{-1}; the fibre undulation was more apparent at 20 mm s^{-1} than 25 mm s^{-1}. When the translation speed was increased to

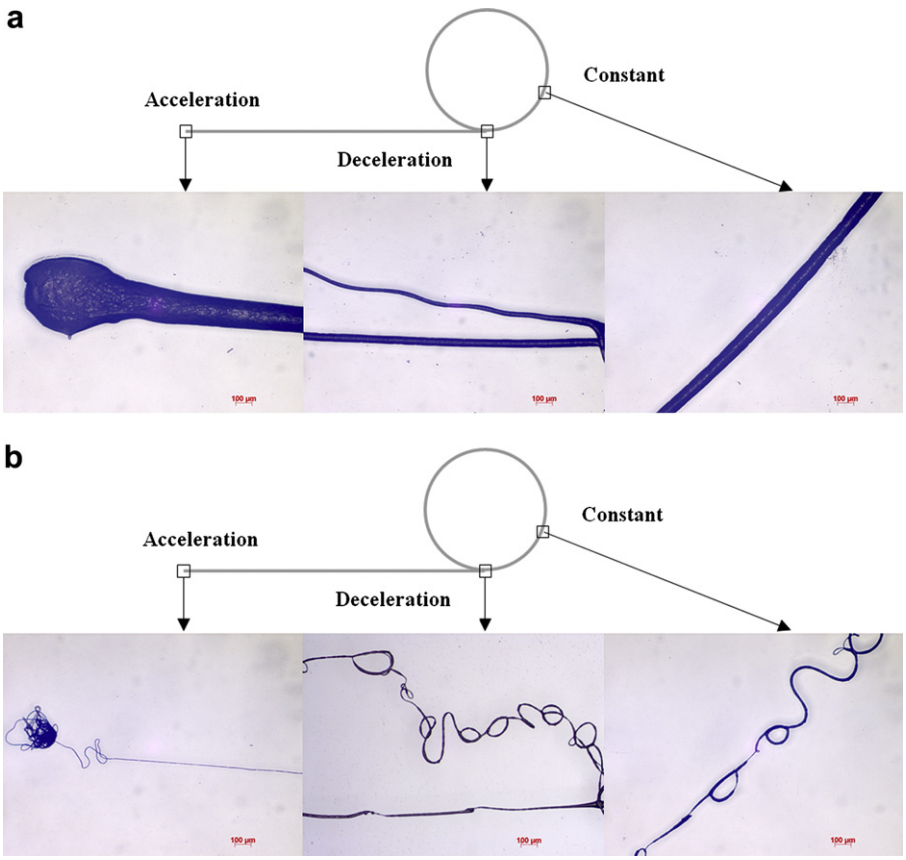

Fig. 5. Optical micrographs showing single jet deposition in the acceleration, constant-speed and deceleration stages in deposition pattern for working distances (a) 1 mm and (b) 5 mm. Experimental parameter settings: 0.8 kV mm^{-1} electric field, 0.3 ml h^{-1} flow rate, 30 mm s^{-1} translation speed. Scale bar: 100 μm.

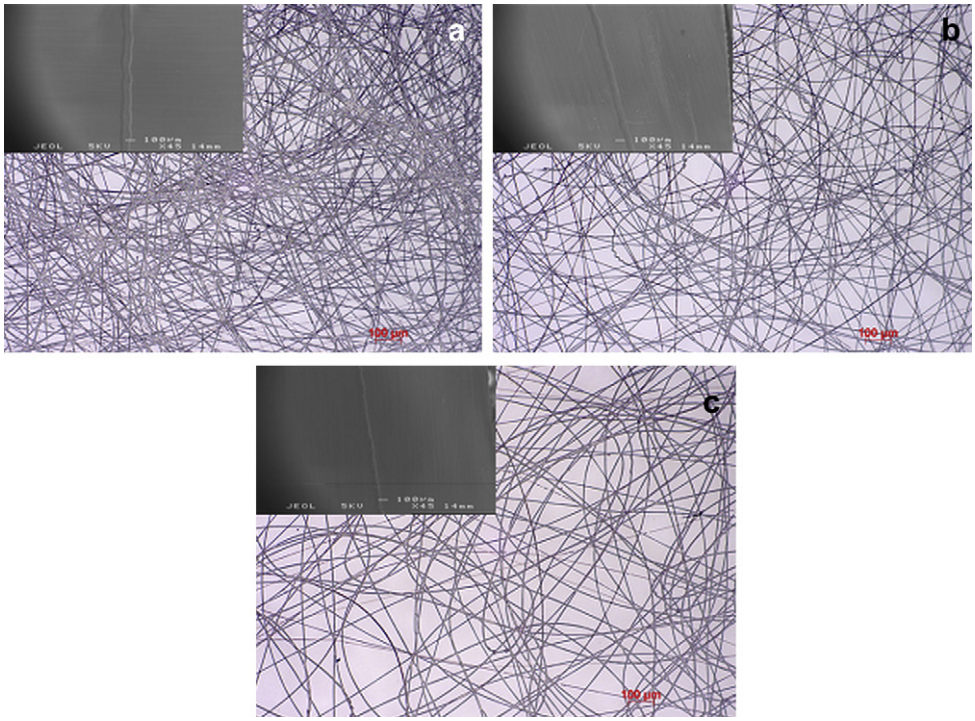

Fig. 6. Optical and SEM micrographs showing the deposition of the sugar-PCL compound jet on a glass slide and an aluminium foil (inset). Spinning conditions: (a) 20 mm s^{-1}, (b) 40 mm s^{-1},and (c) 80 mm s^{-1}. Experimental parameter settings: 5.5 kV applied voltage, 2 cm working distance, 1.0 ml h^{-1} (shell)/0.1 ml h^{-1} (core) flow rates. Scale bar: 100 μm.

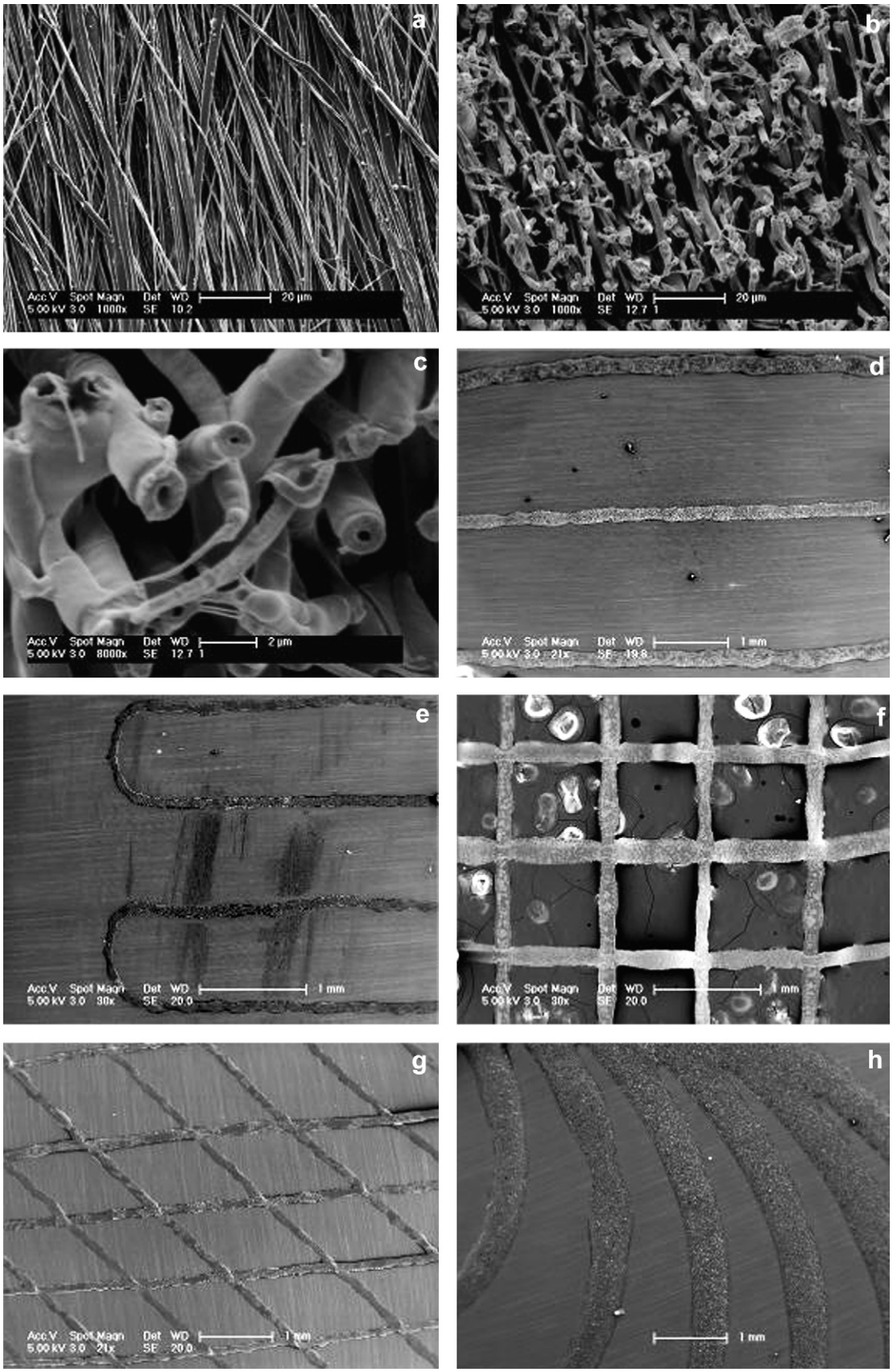

Fig. 7. Typical SEM micrographs of patterned sugar-PCL core–shell fibres: (a–d) aligned parallel to each other (cross-section of aligned fibres in a is shown in b and c), (e) bent, (f) latticed, (g) crossed obliquely and (h) concentrically circular. Coaxial electrospinning conditions: 10.0 kV, 10.0 cm, 3.0 (shell)/0.2 (core) ml h^{-1} for fibres in (a); 5.5 kV, 2 cm, 0.5(shell)/0.05(core) ml h^{-1} for fibres in (d–g); 5.6 kV, 2 cm, 3.0 (shell)/0.2 (core) ml h^{-1} for fibres in (h). Scale bars in a-b, c and d–h: 20, 2 and 1 μm, respectively.

30 mm s^{-1}, the fibre became more linear, indicating that the translation speed was more closely matched to the jet deposition speed. There was a significant decrease in the average diameter of the resultant fibre (from around 32 μm–6 μm) when the translation speed was increased from 20 mm s^{-1} to 45 mm s^{-1}. This diameter decrease can be understood on the basis that the jet is further stretched upon deposition with an increasing translation speed, especially when the translation speed is greater than the jet deposition speed.

3.1.2. Effect of flow rate

Fig. 3 shows that a single fibre was consistently deposited in a linear manner and that this deposition was not influenced by flow rate. The fibre diameter however increased from around 27 μm at 0.03 ml h^{-1} to 80 μm at 0.18 ml h^{-1}. Deterioration of the stability of the jet, due to solution dripping, was noted at higher flow rates.

3.1.3. Effect of working distance

It has already been reported that the fibre deposition pattern changes from a linear path to a random one when the working distance is increased [10]. In this part of our investigation, the working distance was varied between 1 mm and 9 mm, keeping the electric field, flow rate and translation speed constant. A comparison of images of the fibre deposition with a change in working distance is shown in Fig. 4. Clearly the undulation of deposited fibres becomes more pronounced with an increased working distance, which can be explained in terms of an increasing speed mismatch between the jet and the x–y stage collector [10]. It can also be seen that thinner fibres are produced using a higher working distance, where less solvent remains in the jet and more stretching occurs.

Fig. 5 reports a designed deposition pattern (shown schematically above each optical micrograph) and the typical form of the single jet deposition at initial acceleration, constant and deceleration stages during the displacement of the x–y translation along this pattern. When the working distance was set to 1 mm, the jet deposition started with a droplet, followed by a linear fibre with a decreasing diameter in the acceleration stage (Fig. 5a). The diameter of the fibre deposited in a constant-speed stage remained constant, and the fibre tended to undulate in cross-section during the deceleration stage. Fibres were initially deposited in a random manner using a 5 mm working distance, and then became linear, finally buckling in both constant and deceleration stages (Fig. 5b). With further increases in the working distance, the fibre deposition in all three stages exhibited bucking, similar to Fig. 4e and f.

3.2. Deposition of sugar-PCL compound jet

In the case of a single PCL jet, there was no pronounced difference in the deposition on aluminium foil and glass slide substrates. However, when a PCL solution was coaxially electrospun as a shell, with a sucrose solution as the core, the core–shell sugar-PCL fibre deposited on aluminium foil and glass slides in linear (inset SEM images in Fig. 6) and random forms (Fig. 6), respectively. A straight fibre with approximately 100 μm diameter was observed on aluminium foil at a 20 mm s^{-1} translation speed (Fig. 6a inset). By increasing the translation speed, a fibre was deposited in a linear pattern and had a smaller diameter, for example, around 40 μm at 80 mm s^{-1} (Fig. 6c inset). It is interesting that, in all cases, the deposition of a sugar-PCL compound jet on the glass slides was random, comprising thinner fibres. This result is consistent with the observation that the path of the compound jet changed from a straight line to a line comprising straight and spiral states when the deposition substrate changed from aluminium foil to a glass slide. Presumably, the difference in deposition is due to the change in electric field characteristics due to the non-conducting nature of the glass. The sucrose solution is ionic, which might explain the different behaviour of the PCL-only fibres, which, being a polymer has low conductivity [36]. This highlights the ability to control fibre microstructure and deposition patterns by the choice of core solution.

3.3. Patterned sugar-PCL core–shell fibres

To produce patterned core–shell fibres, the x–y stage was used to shift an earthed fibre collector plate covered with aluminium foil along the x and y in-plane axes parallel to the plane of the collector. Fig. 7 shows examples of aligned and patterned sugar-PCL core–shell fibres produced using this setup. Aligned hollow PCL fibres with diameters of around 1.2 μm (Fig. 7a–c) were deposited on the collector using a working distance of 10 cm, where a spiral-like jet was still observed. As shown in Fig. 7d–h, more complex fibre patterns, including parallel, bent, latticed, obliquely crossed and circular were obtained by moving the x–y stage along predetermined trajectories during near-field coaxial electrospinning with a 2 cm working distance. The resultant core–shell fibres (Fig. 7d–g) had much larger average diameters, ranging from 72 to 175 μm, than previously produced samples. The principal reason for this increased diameter is the suppression of the onset of the whipping instability, by using a short working distance, which is essential to control precisely the compound jet deposition; this is much shorter than the 10–20 cm typically used for conventional coaxial electrospinning [10]. Higher flow rates could further increase fibre diameter (Fig. 7h). A special effort is currently being made to produce hollow PCL fibre assemblies having simultaneously the above-mentioned complex patterns and 1–10 μm fibre diameters.

The hollow fibres produced have been specifically designed to have geometrical characteristics similar to the microstructure of neuronal and muscle tissue. The axons found in the white matter of the brain are long, approximately cylindrical, with diameters on the order of 1–10 μm [37]. They are arranged in an aligned pattern within white matter fibre bundles, which may themselves be arranged in arcing, fanning or crossing patterns. The micron scale geometry of coaxial electrospun fibres and their macroscopic arrangements when used with a flexible controlled x–y stage mimic this arrangement (Fig. 7). Similarly, muscle consists of cylindrical structures of a slightly larger diameter [38]. The random mats of cylinders seen in Fig. 6 approximate the less ordered arrangement of cell bodies into a layered structure seen in the grey matter of the brain. These materials, which mimic both the microscopic and macroscopic geometries of tissues, will have applications in medical imaging where controllable materials can provide a ground truth with which to understand imaging signals, with a particular application in diffusion magnetic resonance imaging (MRI).

4. Conclusions

We have comprehensively reported the deposition of PCL single and sugar-PCL compound jets in near-field electrospinning. With an increasing translation speed, the PCL jet deposition changed from a wavy to a linear form, and the fibre width decreased significantly. However, the effect of flow rate was less significant than the other parameters, providing that no solution dripping occurred. The buckling of deposited PCL fibres became pronounced with an increased working distance. In the case of coaxial electrospinning of sugar-PCL solution, it is noted that the compound jet deposition on aluminium foil produced straight and linear fibres, whereas on glass slides, the same spinning conditions produced

random fibre webs. By controlling the x–y stage trajectory and speed, aligned sugar-PCL fibres with diameters of around 1.2 μm were obtained using a long working distance of 10 cm. Complex patterns of sugar-PCL fibres, such as bent, latticed, obliquely crossed and concentrically circular, were produced when the working distance was reduced to 2 cm. These fibres however had much larger diameters ranging from 72 to 175 μm as the bending instability responsible for the formation of thinner electrospun fibres was suppressed and jet stretching reduced significantly.

Acknowledgements

The project "CONNECT" acknowledges the financial support of the Future and Emerging Technologies (FET) programme within the Seventh Framework Programme for Research of the European Commission, under FET-Open grant number: 238292.

References

[1] Teo WE, Ramakrishna S. Nanotechnol 2006;17(14):R89–106.
[2] Greiner A, Wendorff JH. Angew Chem Int Edit 2007;46(30):5670–703.
[3] Reneker DH, Yarin AL, Fong H, Koombhongse S. J Appl Phys 2000;87(9):4531–47.
[4] Yarin AL, Koombhongse S, Reneker DH. J Appl Phys 2001;89(5):3018–26.
[5] Reneker DH, Yarin AL. Polymer 2008;49(10):2387–425.
[6] Bellan LM, Craighead HG. J Vac Sci Technol B 2006;24(6):3179–83.
[7] Liu YQ, Zhang XP, Xia YN, Yang H. Adv Mater 2010;22(22):2454–7.
[8] Sun DH, Chang C, Li S, Lin LW. Nano Lett 2006;6(4):839–42.
[9] Chang C, Limkrailassiri K, Lin LW. Appl Phys Lett 2008;93(12):123111–3.
[10] Hellmann C, Belardi J, Dersch R, Greiner A, Wendorff JH, Bahnmueller S. Polymer 2009;50(5):1197–205.
[11] Rinaldi M, Ruggieri F, Lozzi L, Santucci S. J Vac Sci Technol B 2009;27(4):1829–33.
[12] Zheng GF, Li WW, Wang X, Wu DZ, Sun DH, Lin LW. J Phys D Appl Phys 2010;43(41):415501–6.
[13] Lee SH, Limkrailassiri K, Gao Y, Chang C, Lin LW. Chip-to-chip fluidic connectors via near-field electrospinning. IEEE 20th International Conference on Micro Electro Mechanical Systems. Kobe, Japan; 2007. pp. 61–64.
[14] Chang C, Tran VH, Wang JB, Fuh YK, Lin LW. Nano Lett 2010;10(2):726–31.
[15] Zheng GF, Wang HL, Sun DH, Lin LW. The behaviors of direct-written nanofibers on patterned substrate. 8th IEEE Conference on Nanotechnology; 2008. pp. 179–82.
[16] Wang HL, Zheng GF, Sun DF. Adv Mat Res 2009;60-61:456–60.
[17] Zhou FL, Gong RH, Porat I. Polym Int 2009;58(4):331–42.
[18] Sun Z, Zussman E, Yarin AL, Wendorff JH, Greiner A. Adv Mater 2003;15(22):1929–32.
[19] Loscertales IG, Barrero A, Marquez M, Spretz R, Velarde-Ortiz R, Larsen G. J Am Chem Soc 2004;126(17):5376–7.
[20] Dror Y, Salalha W, Avrahami R, Zussman E, Yarin AL, Dersch R, et al. Small 2007;3(6):1064–73.
[21] Moghe AK, Gupta BS. Polym Rev 2008;48(2):353–77.
[22] Wang C, Yan KW, Lin YD, Hsieh PCH. Macromolecules 2010;43(15):6389–97.
[23] Zhang H, Zhao CG, Zhao YH, Tang GW, Yuan XY. Sci China Chem 2010;53(6):1246–54.
[24] Zhang L, Wang K, Zhao Q, Zheng WT, Wang ZH, Wang SF, et al. Sci China Chem 2010;53(3):528–34.
[25] Chan KHK, Nakagawa R, Kotaki M. J Text Eng 2010;56(1):9–13.
[26] Muthiah P, Hsu SH, W. S. Langmuir 2010;26(15):12483–87.
[27] Zhang YZ, Wang X, Feng Y, Li J, Lim CT, Ramakrishna S. Biomacromolecules 2006;7(4):1049–57.
[28] Lee G, Song JC, Yoon KB. Macromol Res 2010;18(6):571–6.
[29] Yu JH, Fridrikh SV, Rutledge GC. Adv Mater 2004;16(17):1562–6.
[30] Wang M, Yu JH, Kaplan DL, Rutledge GC. Macromolecules 2006;39(3):1102–7.
[31] Xin Y, Huang Z, Li W, Jiang Z, Tong Y, Wang C. Euro Polym J 2008;44(4):1040–5.
[32] Ou KL, Chen CS, Lin LH, Lu JC, Shu YC, Tseng WC, et al. Eur Polym J 2011;47(5):882–92.
[33] Xie J, MacEwcm MR, Willerth SM, Li X, Moran DW, Sakiyama-Elbert SE, et al. Adv Funct Mater 2009;19(14):2312–8.
[34] Liao IC, Chew SY, Leong KW. Nanomedicine 2006;1(4):465–71.
[35] Miyauchi M, Miao JJ, Simmons TJ, Lee JW, Doherty TV, Dordick JS, et al. Biomacromolecules 2010;11(9):2440–5.
[36] Enayati M, Ahmad Z, Stride E, Edirisinghe M. J R Soc Interface 2010;7(Suppl. 4):S393–402.
[37] Poupon C, Rieul B, Kezele I, Perrin M, Poupon F, Mangin JF. Magn Reson Med 2008;60(6):1276–83.
[38] Potter RF, Groom AC. Microvasc Res 1983;25(1):68–84.